Evaluation of Basic Amphipathic Peptides for Cellular Delivery of Antisense Peptide Nucleic Acids

Martin A. Maier,* Christine C. Esau, Andrew M. Siwkowski, Edward V. Wancewicz, Klaus Albertshofer, Garth A. Kinberger, Neena S. Kadaba, Tanya Watanabe, Muthiah Manoharan, C. Frank Bennett, Richard H. Griffey, and Eric E. Swayze

Department of Medicinal Chemistry, Isis Pharmaceuticals, Inc., 1891 Rutherford Road, Carlsbad, California 92008

Received December 21, 2005

Cellular permeation peptides have been used successfully for the delivery of a variety of cargoes across cellular membranes, including large hydrophilic biomolecules such as proteins, oligonucleotides, or plasmid DNA. For the present work, a series of short amphipathic peptides was designed to elucidate the structural requirements for efficient and nontoxic delivery of peptide nucleic acids (PNAs). On the basis of an idealized α-helical structure, the helical parameters were modulated systematically to yield peptides within a certain range of hydrophobicity and amphipathicity. The corresponding PNA conjugates were synthesized and characterized in terms of secondary structure, enzymatic stability, and antisense activity. The study revealed correlations between the physicochemical and biophysical properties of the conjugates and their biological activity and led to the development of potent peptide vectors for the cellular delivery of antisense PNAs. Two representative compounds were radiolabeled and evaluated for their biodistribution in healthy mice.

Introduction

Peptide nucleic acids (PNAs), which were developed by Nielsen, Buchardt, and co-workers more than a decade ago, are nucleic acid analogues with an achiral, uncharged polyamide backbone.[1] Their high binding affinity to complementary DNA or RNA mediated by Watson−Crick base pairing[2] and their extraordinary stability against enzymatic degradation make them attractive candidates for antisense and antigene applications.[3] However, limited solubility in physiological buffers, insufficient cellular uptake, and poor biodistribution due to rapid elimination and excretion have thus far prevented the broad application of unmodified PNA in vitro as well as in vivo. Furthermore, peptide nucleic acids do not support RNase H-mediated cleavage of mRNA transcript,[4] which has been shown to be the predominant mechanism of action for DNA-like antisense oligonucleotides.[5] Therefore, a viable antisense strategy involving PNA-based inhibitors has to rely on alternative mechanisms such as alteration of pre-mRNA splicing, translational arrest, or inhibition of transcription. The latter has been reinvestigated recently by Corey and co-workers, who demonstrated that PNAs targeting transcriptional start sites can be potent and specific inhibitors of gene expression.[6]

We previously have identified a peptide nucleic acid that is capable of efficiently redirecting splicing of murine CD40 mRNA, thereby inhibiting CD40 expression.[7] CD40 is a membrane protein that is expressed on antigen-presenting cells such as B lymphocytes, dentritic cells, and macrophages. Its role in the initiation and propagation of inflammation suggests that inhibition of CD40 signaling could be therapeutically relevant for inflammatory and autoimmune diseases.[8,9]

On the basis of earlier studies with Kole and co-workers,[10,11] we discovered that a simple octa(L-lysine) motif is capable of promoting free uptake of PNAs into mouse BCL_1 cells as well as primary murine macrophages.[7] A subsequent SAR study revealed a strong correlation between the number and type of cationic headgroups and the observed antisense activity under conditions of 'free' cellular uptake, i.e., without the aid of transfection agents or electroporation.[12]

To date, a wide variety of cell-penetrating peptides (CPPs) have been reported to promote cellular uptake of various cargo molecules ranging from proteins to nucleic acids (for reviews on cell-penetrating peptides, see refs 13−15). However, the mechanisms by which these CPPs cross the plasma membrane and enter the cells are not well understood. Diverse and sometimes controversial findings are reported, which suggests that multiple pathways could be involved in the process of internalization. Hence, one can conclude that the degree at which each pathway contributes to the overall uptake and intracellular distribution will depend on a variety of factors, including the structure of the peptide itself, its cargo, the cell type, and the experimental conditions. Recently for instance, this has been reviewed comprehensively for the HIV Tat-derived basic peptide.[16]

Amphipathic model peptides offer an attractive starting point for systematic SAR studies. Their physicochemical properties can be easily and rationally modulated through changes in their amino acid sequence. Using a series of lysine-rich amphipathic model peptides, the effect of structural changes, such as peptide length, charge, and helix parameters, on the magnitude and mechanism of cellular uptake was investigated by Oehlke and co-workers.[17] The authors reported that besides a minimum length and an overall positive net charge, helical amphipathicity was the only essential parameter for efficient cellular uptake. Later they found that the cellular enrichment of amphipathic peptides in contrast to their nonamphipathic counterparts was due to reduced efflux of the peptides rather than enhanced uptake.[18] An amphipathic model octadecamer peptide covalently linked to a PNA that targets the rat nociceptin/orphanin FQ receptor was found to increase intracellular concentration 3−8-fold and improve the biological activity in cultured cells 5-fold compared to the unmodified PNA.[19] More recently, a PNA directed against the HIV TAR apical loop was shown to inhibit Tat-dependent *trans*-activation, when conjugated to various CPPs either through an enzymatically stable linker or via a cleavable disulfide.[20] The activity of the conjugates as well as

* To whom correspondence should be addressed. Phone: 760-603-2334. Fax, 760-603-4657. E-mail, mmaier@isisph.com.

10.1021/jm051275y CCC: $33.50
Published on Web 03/22/2006

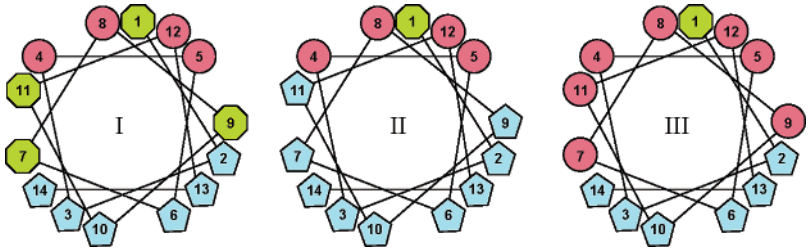

Figure 1. Helical wheel projections of the three different groups of peptides. Basic amino acids are depicted as blue pentagons, hydrophobic amino acids as red circles, and anionic or neutral−polar amino acids as green octagons.

the cell uptake pattern was found to vary significantly with the type of peptide used. In some cases, the presence of the lysosomotropic reagent chloroquine substantially enhanced or accelerated the inhibitory effect, suggesting that entrapment of the conjugates in endosomal or membrane compartments limited the activity of those compounds.

For the present study, we designed a series of small basic peptides based on a simple helical−amphipathic motif and evaluated the structural features required for effective cellular delivery of a PNA targeting murine CD40. The antisense activity of the PNA conjugates, being an unambiguous measure for effective nuclear delivery, was used as the primary endpoint of the study. While the first set of compounds was evaluated in a mouse B-cell lymphoma cell line, the follow-up study with one of the most promising motifs was performed in primary mouse macrophages. In addition, the effect of the structural modifications on enzymatic stability and cell viability was investigated. A few representative examples of the series of conjugates were evaluated for their PK/tissue distribution in healthy mice.

Results and Discussion

The antisense PNA used in this study targets the 3′-end of exon 6 of the primary murine CD40 transcript. We have previously established that the unmodified version bearing just a single L-lysine residue at the C-terminus (**1**) can promote the omission of exon 6 from CD40 pre-mRNA in a sequence- and dose-dependent fashion, which leads to a frame shift in the downstream codons of exon 7, 8, and 9 and truncates the protein due to an in-frame stop codon in exon 8.[7] The induced splice variant matches an alternatively spliced transcript of murine CD40 (type 2), which occurs naturally at low abundance and lacks the sequence encoding for the transmembrane domain.[21] Our preliminary experiments showed that conjugating **1** to short oligolysine peptides significantly improved activity under conditions of free cellular uptake, i.e., without the use of facilitated delivery such as electroporation. In particular, the potency of an octa(L-lysine) conjugate **2** after free uptake was comparable to the unmodified PNA **1** delivered by electroporation. A more detailed study based on this simple cationic peptide motif revealed some of the structural features required for effective cellular delivery.[12]

The antisense PNA used in the present as well as the previous studies operates through modulation of splicing. To reach its target pre-mRNA, it must be able to (i) bind to the cell surface and trigger cellular uptake, (ii) cross the lipid bilayer and enter the cytoplasm, (iii) translocate to the nucleus, and (iv) bind to its target pre-mRNA at a specific site and inhibit the splicing machinery. In contrast to the majority of studies involving cell penetrating peptides, the purpose of the present work was to identify the structural features required for a short amphipathic peptide vector to not only mediate transport of the PNA through the plasma membrane but to deliver it to its pre-mRNA target in the nucleus. Thus, the ability of the corresponding PNA−peptide conjugates to alter splicing of CD40 transcript and inhibit expression of membrane-bound CD40 protein was considered the primary endpoint of this study. The compounds were also evaluated in terms of secondary structure and enzymatic stability.

First Tier SAR Study. On the basis of an idealized α-helical structure, a series of short amphipathic peptides was designed through alterations of the amino acid composition of both helical faces to cover a range of the helix parameters hydrophobicity and amphipathicity. The following rules were applied for the first tier of compounds: (i) constant peptide length of 14 amino acids, which corresponds to approximately 3.5 helical turns; (ii) assuming an α-helical structure, the peptides contain a hydrophobic face and a hydrophilic face optionally linked by neutral−polar (glycine, glutamine) or acidic residues (glutamic acid); (iii) the hydrophilic face only contains the basic amino acids lysine or arginine; and (iv) the hydrophobic face only contains the residues alanine, leucine, phenylalanine, and tryptophan in various combinations. All peptides were attached to the N-terminus of the PNA via an 8-amino-3,6-dioxaoctanoic acid linker (O-spacer).

On the basis of their composition, the peptides of this study can be divided into three different groups (Figure 1 and Table 1). Peptides of group I contain neutral−polar or anionic residues bridging the two faces of the helix, while the peptides of group II and III contain an extended hydrophilic/cationic face and an extended hydrophobic face, respectively. Group I and II peptides both display low hydrophobicity and amphipathicity, due to the small number of hydrophobic amino acids and a narrow hydrophobic face, respectively. Extending the hydrophobic face (group III) leads to an increase in both the hydrophobicity as well as the amphipathicity of the peptides, ranging from moderate values for the alanine/leucine combination of **8** to high values for the leucine/phenylalanine and the tryptophan/phenylalanine combination of **9** and **10**, respectively.

Among conjugates with equal numbers of basic residues, changes in the theoretical hydrophobicity values generally correlated well with corresponding shifts in the HPLC retention times (see Table 1, groups I and III). Due to the mode of separation by ion-pairing with heptafluorobutyrate, however, the lysine- or arginine-rich conjugates of group II displayed a higher retention time than expected from their calculated helix parameters.

Structural analysis of the conjugates by CD spectroscopy demonstrated that the small, highly charged amphipathic peptides generally showed a low tendency to form ordered structures at neutral pH, due to charge repulsion between the protonated basic residues (Table 1). While little effect was seen for the peptides of groups I and II, the presence of the negatively charged detergent SDS induced the formation of α-helical structure in peptides of group III with an extended hydrophobic face. This is exemplified for compound **8** in Figure 2 showing

Table 1. First Tier SAR: Sequence, HPLC Retention Time, and Helix Parameters of the Amphipathic Peptides

PNA conjugate	group	peptide sequence (N to C)	t_R[a]	⟨*H*⟩[b]	⟨μH⟩[c]	$[\theta]_r$[d] × 10^{-4} pH 7	$[\theta]_r$[d] × 10^{-4} pH 7/SDS
3	I	GKKAFKGAGKGFKK	20.9	−0.124	0.54	0.52	0.4
4	I	GRRAFRGAGRGFRR	21.0	−0.133	0.55	0.1	0.1
5	I	GKKAFKEAEKGFKK	20.3	−0.216	0.56	0.45	0.12 −0.9 (pH 5)
6	II	GKKAFKKAKKKFKK	21.0	−0.336	0.56	0.45	0
7	II	GRRAFRRARRRFRR	21.9	−0.349	0.56	0.4	N/A
8	III	GKKALKLAAKLLKK	21.9	0.128	0.54	0.1	−2.2
9	III	GKKLFKLFLKLFKK	23.1	0.445	0.71	0.25	−2.0
10	III	GKKWFKWFWKFFKK	23.4	0.569	0.73	N/A	N/A

[a] Retention time on Zorbax SB300 C_3 column (Agilent) using 0.1% heptafluorobutyric acid in H_2O and CH_3CN as eluents A and B, respectively. [b] Mean hydrophobicity per residue (Fauchère and Pliška). [c] Mean hydrophobic moment per residue. [d] Mean residue ellipticity at 220 nm.

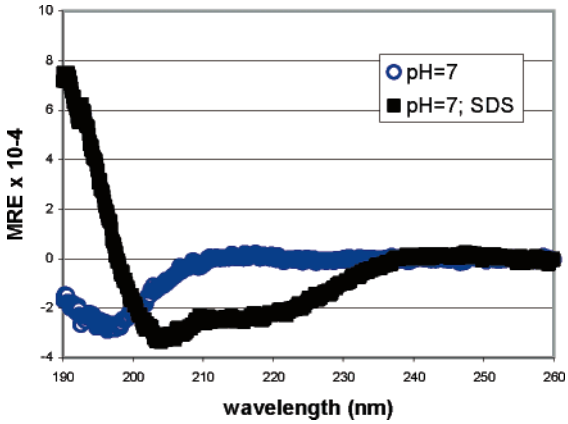

Figure 2. CD spectroscopy of compound **8**. Mean residue ellipticity (MRE) as a function of wavelength; PBS buffer, pH 7 without (open blue circles) and with 15 mM SDS (black squares).

the characteristic minimum at 220 nm in SDS-containing buffer but not under SDS-free conditions. In case of **5**, SDS-induced helix formation occurred only at acidic pH (pH 5), at which the glutamic acid residues were partially protonated.

The results indicate that despite similar amphipathicities, the presence of helix-destabilizing glycine residues (group I) or charge repulsion within an extended face of positively charged residues (group II) substantially reduced the propensity of helix formation.

The PNA−peptide conjugates were screened under conditions of free uptake in BCL_1 cells, a murine B-cell lymphoma cell line that constitutively expresses high levels of CD40 (Table 2). CD40 cell-surface expression was analyzed by flow cytometry. Cell viability was assessed by WST-1 assay and cytotoxicity was considered significant if the level of viable cells dropped below 50% of the untreated control following 3 days of compound exposure. It should be pointed out that during this period the untreated cells go through at least two cell divisions. Therefore, the assay provides a very sensitive readout of cell viability, albeit without distinguishing between cytotoxic and cytostatic effects. It has been previously reported that cationic lysine-tagged PNAs can exhibit nonspecific electrostatic interactions with DNA under low-salt conditions, which causes the rates of sequence-specific binding to slow substantially.[22] This effect, however, has been found to be negligible under higher (physiological) salt concentrations. In fact, we have demonstrated that a four-base mismatch control bearing the octa(L-lysine) peptide showed no effect on CD40 expression and both the octa(L-lysine) conjugate **2** and its unmodified parent **1** displayed similar potency, when electroporated into the cells.[7] Nevertheless, nonspecific binding to polyanionic DNA or RNA cannot be completely ruled out if highly cationic PNAs, such as the ones described in this work, are used for biological applications and it could in part relate to the observed cytotoxicity. The enzymatic stability of the conjugates was evaluated in serum-containing cell culture medium and 25% mouse serum. Therefore, the compounds were analyzed by HPLC after removal of serum proteins by precipitation as reported previously.[12]

The octa(L-lysine) conjugate **2** and a conjugate bearing the known cellular permeation peptide HIVtat (**11**) were used as positive controls in this experiment. The conjugates of group I generally displayed only little activity. Some improvement could be observed by replacing the lysine residues of **3** with arginines (**4**), while the incorporation of glutamic acids (**5**) completely abolished activity. Both conjugates of group II (**6**, **7**) showed a robust reduction of CD40 protein expression that was comparable or even better than for the positive controls **2** and **11** bearing the octa(L-lysine) and the HIVtat peptide, respectively. Robust activity was also observed with conjugate **8** of group III. The other, more amphipathic, peptides of this group (**9** and **10**) were essentially inactive at the lowest concentration (1 μM) and displayed severe cytotoxicity at higher concentrations. Considering that their hydrophobicities and hydrophobic moments lie well within the range of various toxic peptides, which are known to cause destabilization of cellular membranes, these findings are not unexpected.[23]

The enzymatic stability of the peptide part of the conjugates was found to vary considerably. Generally, the lysine-rich conjugates **3** and **6** exhibited 100-fold higher half-lives in 10% FBS than their corresponding arginine analogues **4** and **7**, respectively. This difference in stability was also observed, albeit less pronounced, in 25% mouse serum with half-lives being about 4−10-fold higher for the lysine peptides. Interestingly, the two most hydrophobic peptide conjugates **9** and **10** displayed higher than expected half-lives in mouse serum. We observed that in mouse serum both conjugates were highly bound to serum proteins, suggesting that their improved enzymatic stability was due to the reduced fraction of "free" compound.

The enzymatically stabile isomers (all D-amino acids) of the three most active conjugates **6**−**8** were prepared with the same (inverso isomer, **12**−**14**) or the reversed sequence (retro-inverso isomer **15**−**17**). Between the two D-isomers of each sequence, no significant differences in activity or toxicity were found. This indicates that within a given peptide sequence, the orientation of the side chains did not play a significant role in the process of internalization and intracellular trafficking. While the stabilization of the peptide backbone appeared to improve activity of the arginine-rich peptide conjugates (**13**, **16**) compared to their parent (**7**), no significant improvement was observed for the lysine-rich D-isomers **12**, **14** and **15**, **17** compared to their L-isomers **6** and **8**, respectively. This correlates with a higher

Table 2. First Tier PNA−Peptide Conjugates: Effect on Antisense Activity, Cell Viability, and Enzymatic Stability

compd	peptide sequence on the N-terminus (N) and C-terminus (C) of the PNA	activity (% UTC)[a] 10 μM	3 μM	1 μM	cell viability (μM)[b]	half-life ($t_{1/2}$) 10% FBS	25% MS
1	K (C)	96 ± 1	95 ± 0	99 ± 1	>20	n/a[c]	n/a
2	K_8 (N), K (C)	38 ± 3	72 ± 3	78 ± 6	10−20	≫7 d[d]	6.7 ± 1.4 h
3	GKKAFKGAGKGFKK (N), K (C)	65 ± 7	72 ± 4	80 ± 3	>20	ca. 200 h	0.9 h
4	GRRAFRGAGRGFRR (N), K (C)	46 ± 3	70 ± 1	70 ± 6	>20	2 h	0.1 h
5	GKKAFKEAEKGFKK (N), K (C)	83 ± 6	85 ± 10	97 ± 5	>20	≫7 d[d]	2.3 h
6	GKKAFKKAKKKFKK (N), K (C)	28 ± 5	39 ± 12	74 ± 5	10	∼130 h	0.4 h
7	GRRAFRRARRRFRR (N), K (C)	25 ± 1	66 ± 3	89 ± 3	10−20	1 h	0.1 h
8	GKKALKLAAKLLKK (N), K (C)	33 ± 2	78 ± 4	95 ± 1	>20	∼200 h	0.9 h
9	GKKLFKLFLKLFKK (N), K (C)	n/a	n/a	86 ± 4	1.25−2.5	∼100 h	4 h
10	GKKWFKWFWKFFKK (N), K (C)	n/a	n/a	81 ± 12	1.25−2.5	∼100 h	3.6 h
11	GRKKRRQRRRG (N), K (C)	39 ± 2	62 ± 5	84 ± 2	>20	3.5 h	0.4 h
12	D-(GKKAFKKAKKKFKK) (N), K (C)	n/a	41 ± 3	79 ± 10	2.5−5	≫7 d	≫48 h[d]
13	D-(GRRAFRRARRRFRR) (N), K (C)	n/a	25 ± 3	84 ± 7	2.5	≫7 d	≫48 h
14	D-(GKKALKLAAKLLKK (N), K (C)	41 ± 1	76 ± 3	89 ± 1	20	≫7 d	≫48 h
15	D-(KKFKKKAKKFAKKG) (N), K (C)	n/a	39 ± 2	76 ± 3	2.5−5	≫7 d	≫48 h
16	D-(RRFRRRARRFARRG) (N), K (C)	n/a	28 ± 3	82 ± 10	2.5	≫7 d	≫48 h
17	D-(KKLLKAALKLAKKG) (N), K (C)	35 ± 2	80 ± 6	89 ± 9	20	≫7 d	≫48 h

[a] Inhibition of CD40 expression in BCL_1 cells treated with PNA conjugates at concentrations of 10, 3, and 1 μM and analyzed by flow cytometry. The values shown represent the averages ± SD of percent untreated control ($n = 3$). [b] Concentration at which cell viability (measured by WST-1 assay) dropped below 50% of untreated control. [c] No degradation observed within the period of time indicated. [d] No data available.

Table 3. Second Tier SAR: Sequence, HPLC Retention Time, and Helix Parameters of the Amphipathic Peptides

PNA conjugate	peptide sequence on the N-terminus (N) and C-terminus (C) of the PNA	t_R[a]	$\langle H \rangle$[b]	$\langle \mu H \rangle$[c]
8	GKKALKLAAKLLKK (N), K (C)	21.9	0.128	0.54
18	GHKALKLAAKLLKH (N), K (C)	22.3	0.288	0.46
19	GKKALHLAAHLLKK (N), K (C)	22.1	0.288	0.39
20	GKHALKLAAKLLKH (N), K (C)	22.4	0.288	0.47
21	GHKALKLAAKLLHH (N), K (C)	22.5	0.368	0.40
22	GKHALHLAAHLLKK (N), K (C)	22.2	0.368	0.34
23	GKKALHLAAHLLKH (N), K (C)	22.1	0.368	0.37
24	GRRALRLAARLLRR (N), K (C)	23.1	0.119	0.55
25	WHKALKALFKLLKH (N), K (C)	23.8	0.554	0.74
26	WKHALKALFKLLKH (N), K (C)	23.8	0.554	0.70
27	WHKALHALFHLLKH (N), K (C)	23.1	0.714	0.60
28	GKKALKALFKLLKK (N), K (C)	23.3	0.234	0.66

[a] Retention time on Zorbax SB300 C_3 column (Agilent) using 0.1% heptafluorobutyric acid in H_2O and CH_3CN as eluents A and B, respectively. [b] Mean hydrophobicity per residue (Fauchère and Pliška). [c] Mean hydrophobic moment per residue.

enzymatic stability observed for the L-lysine-rich peptides compared to the L-arginine-rich ones. The D-isomers **12**, **13**, **15**, and **16** displayed a significant increase in cytotoxicity, which is probably due to the substantially increased half-lives of their highly basic peptide motifs, which would be otherwise more rapidly degraded by proteases present in the cell culture medium as well as inside the cells. On the other hand, the stabilization of the less basic conjugate **8** did not affect cell viability (**14**, **17**).

Second Tier SAR Study. Two features essential for efficient delivery of the PNA cargo became apparent from the first tier SAR study: net positive charge and amphipathicity. A modest increase in hydrophobicity and amphipathicity, enhanced activity; more dramatic changes, however, substantially increased the cytotoxicity of the compounds. For the second tier SAR study, we focused on the peptide motif of **8**, the only representative of the more hydrophobic group III found to promote efficient cellular uptake of the corresponding conjugate without concomitant increase in cytotoxicity. The helical parameters hydrophobicity and amphipathicity were gradually varied by replacing selected residues in both faces of the helix (Table 3).

Two or three lysine residues were replaced with histidine at various positions in compounds **18**−**20** and **21**−**23**, rendering peptides with increased hydrophobicity but reduced amphipathicity. The histidine-containing conjugates with their lower net positive charge at neutral pH were designed to reduce membrane activity and cytotoxicity. However, in more acidic compartments of the cell, the imidazolyl side chains will be protonated, restoring the ability of the peptides to interact with the lipid bilayer. Histidine-rich peptides have been reported previously for transfection of negatively charged oligonucleotides into cells, and their transfection efficiency has been found to be pH-dependent.[24]

Compound **24**, in which all the lysine residues were replaced with arginine, has very similar theoretical helix parameters as its parent conjugate **8**. Changes in both faces of the helix were made in compounds **25**−**27**, which led to significant increases in both hydrophobicity and amphipathicity. As a reference, compound **28** was only modified in the hydrophobic face of the helix by replacing the alanine in position 9 with the more hydrophobic phenylalanine and switching the positions of leucine-7 and alanine-8. This change caused a moderate increase in hydrophobicity as well as amphipathicity.

As in the first tier SAR, changes in the theoretical values for hydrophobicity and amphipathicity generally correlated with corresponding shifts in the HPLC retention time. Exceptions were the arginine-rich conjugate **24** and the lysine-containing **28**, which both showed higher than expected retention times. In the case of **24**, the increase, which had been also observed for conjugate **7** compared to **6**, appeared to be due to the stronger ion-pairing properties of arginine compared to lysine. On the other hand, the retention time of **28**, which was higher than expected from its moderate hydrophobicity, appears to be due to its elevated amphipathicity, which is in the same range as the values for conjugates **24**−**27**.

Structural investigations using CD spectroscopy demonstrated an increased propensity of the histidine-rich conjugate **27** to form an α-helical structure at pH 7 with a mean residue ellipticity (MRE) at 220 nm of −1.0 compared to 0.70 at pH 5 (Supporting Information). The effect was further enhanced in the presence of SDS. The observed pH-dependence demonstrates, in accordance with the previous results, how charge repulsion between the basic residues of the hydrophilic face can reduce the propensity for helix formation.

To expand our studies to a nontransformed cell line, primary murine macrophages were used to evaluate this second set of conjugates, together with the unmodified PNA **1**, the parent

Table 4. Second Tier PNA−Peptide Conjugates: Effect on Antisense Activity and Cell Viability

compd	downregulation of type 1 CD40 mRNA (%UTC) [a]			upregulation of type 2 CD40 mRNA (%UTC)[b]			cell viability (μM)[c]
	6 μM	3 μM	1.5 μM	6 μM	3 μM	1.5 μM	
1	50 ± 10	61 ± 3	74 ± 12	300 ± 60	320 ± 14	310 ± 10	>6
8	14 ± 3	38 ± 0.5	69 ± 7	790 ± 160	770 ± 70	470 ± 30	6
14	2 ± 1	6 ± 1	21 ± 3	1680 ± 750	2740 ± 490	2190 ± 380	6
17	1 ± 0	3 ± 1	14 ± 1	1100 ± 110	1870 ± 70	1990 ± 500	6
18	38 ± 10	53 ± 6	60 ± 9	350 ± 90	290 ± 40	200 ± 20	>6
19	51 ± 10	59 ± 10	63 ± 12	370 ± 50	250 ± 30	180 ± 20	>6
20	41 ± 10	67 ± 10	61 ± 10	450 ± 100	360 ± 50	190 ± 50	>6
21	63 ± 6	60 ± 23	62 ± 3	420 ± 40	200 ± 80	166 ± 4	>6
22	56 ± 14	77 ± 25	70 ± 9	300 ± 90	310 ± 70	220 ± 30	>6
23	56 ± 14	70 ± 24	73 ± 17	520 ± 250	320 ± 90	250 ± 50	>6
24	24 ± 7	52 ± 7	69 ± 13	1580 ± 340	1020 ± 290	480 ± 180	>6
25	16 ± 4	76 ± 12	109 ± 27	170 ± 40	190 ± 40	170 ± 60	3−6
26	13 ± 4	80 ± 16	107 ± 13	233 ± 81	354 ± 92	230 ± 51	3−6
27	11 ± 1	47 ± 5	91 ± 25	798 ± 35	686 ± 101	604 ± 154	6
28	8 ± 5	49 ± 3	80 ± 18	147 ± 95	542 ± 119	525 ± 225	3

[a] Downregulation of CD40 type 1 mRNA in primary murine macrophages treated with PNA conjugates at concentrations of 6, 3, and 1.5 μM and analyzed by RT-PCR. The values shown represent the averages ± SD of percent untreated control ($n = 3$). [b] Corresponding upregulation of the alternatively spliced product (type 2 mRNA). [c] Concentration at which total RNA (measured by ribogreen assay) dropped below 50% of untreated control.

conjugate **8**, and its stabilized analogues **14** and **17**. After incubation with PNA conjugates, the cells were activated with rINF-γ to induce CD40 expression. The antisense activity of the conjugates was measured by RT-PCR of the CD40 transcript (type 1) and its alternatively spliced form (type 2). Cell viability was assessed by measuring the effects on total RNA using a ribogreen assay (Table 4).

The unmodified PNA **1** showed some moderate activity in reducing the predominant CD40 type 1 transcript by about 50%. However, the reduction of type 1 was not accompanied with a corresponding increase in type 2 transcript, indicating that the observed effect was not due to induction of alternative splicing. The parent conjugate **8** displayed concentration-dependent reduction of type 1 as well as induction of the type 2 transcript. At 6 μM concentration, however, cytotoxicity became evident from the reduction in total RNA as well as the lower than expected increase in type 2 transcript. Interestingly, the enzymatically stable analogues **14** and **17** were significantly more potent than the parent compound without additional impact on cell viability.

As found in the first SAR series, reducing the net positive charge of the conjugates, in this case by replacing lysine residues with histidines while leaving the hydrophobic face unchanged, led to a significant decrease in activity, regardless of the positions replaced (**18**−**23**). On the other hand, **24**, the all-arginine analogue of **8**, was found to have comparable activity and reduced cytotoxicity, as evident from the concentration-dependent decrease in type 1 transcript and corresponding increase in type 2 transcript.

With conjugates **25**−**27** we attempted to balance the decrease in charge and the corresponding loss in activity with an increase in hydrophobicity and amphipathicity. Bolstering the hydrophobic face of the helix, however, seemed to exacerbate the cytotoxicity of the conjugates rather than improve the potency. This trend toward higher cytotoxicity was also observed with conjugate **28**, in which the hydrophilic face was unchanged and the hydrophobic face was rearranged to achieve a moderate increase in hydrophobicity and amphipathicity. Only **27**, with four of the six lysines replaced with histidines, was comparable to the parent conjugate **8** in terms of activity and cytotoxicity.

The results confirm the findings of the first tier SAR and suggest that the tolerated range of amphipathicity is narrow and one has to carefully balance the composition of the peptide with regard to the ratio of hydrophobic and basic amino acids in the two faces of the helix. The most significant improvement in activity was obtained by stabilizing the peptide backbone. Both D-isomers **14** and **17** were clearly more potent than the parent conjugate **8** without a concomitant increase in toxicity. Considering that the antisense activities of the three conjugates were comparable in BCL_1 cells (Table 2), the observed differences in macrophages could be due to altered rates of intracellular metabolism, possibly combined with efficient efflux of the degradation products.[25]

Cellular Uptake. To determine gross differences in their cellular uptake/association, primary murine macrophages were incubated with the fluorescently labeled versions of the unmodified PNA **1**, conjugate **8**, its enzymatically stabilized analogue **17**, and the histidine-rich, hydrophobic analogue **27** and evaluated by fluorescence microscopy (Figure 2, Supporting Information). After 6 h of incubation at concentration of 3 and 6 μM, the unmodified PNA **1** did not show any evidence of cell association. The peptide conjugate **8** was found to be associated with a fraction of the cells but only at the highest concentration (6 μM). In contrast, both **17** and **27** showed intense staining of the majority of the cells at 3 μM concentration.

Comparing the parent conjugate **8** with histidine-rich analogue **27**, it appears that uptake and activity are not as closely correlated as one might expect. On one hand, the potency of the conjugates clearly depends on the ability of the peptides to penetrate the lipid bilayer and to survive enzymatic attack. But then the peptide carrier not only mediates cellular uptake and escape from an endosomal pathway but likely influences the intracellular trafficking as for instance the accumulation of the conjugate in the nucleus. Several short, highly basic peptide sequences have been identified as nuclear localization signals mediating the recognition and nuclear transport by various shuttling proteins (for review see ref 26). Thus, possible explanations for the observed discrepancy between uptake and activity of **27** are a less efficient escape from endosomal/lysosomal vesicles and/or diminished nuclear accumulation due to substantially reduced lysine content. In contrast, the enhanced cellular uptake of **17** compared to **8** correlates well with the observed improvement in activity and underlines the importance of enzymatic stability.

To elucidate further the mechanism of uptake, an octa(L-lysine) PNA−conjugate (**29**) with a sequence unrelated to the CD40 target ((L-Lys)$_8$-TCTCAGCACATCTACA-Lys) was used to determine whether the cellular uptake occurs through an easily saturable mechanism and whether different peptides utilize the

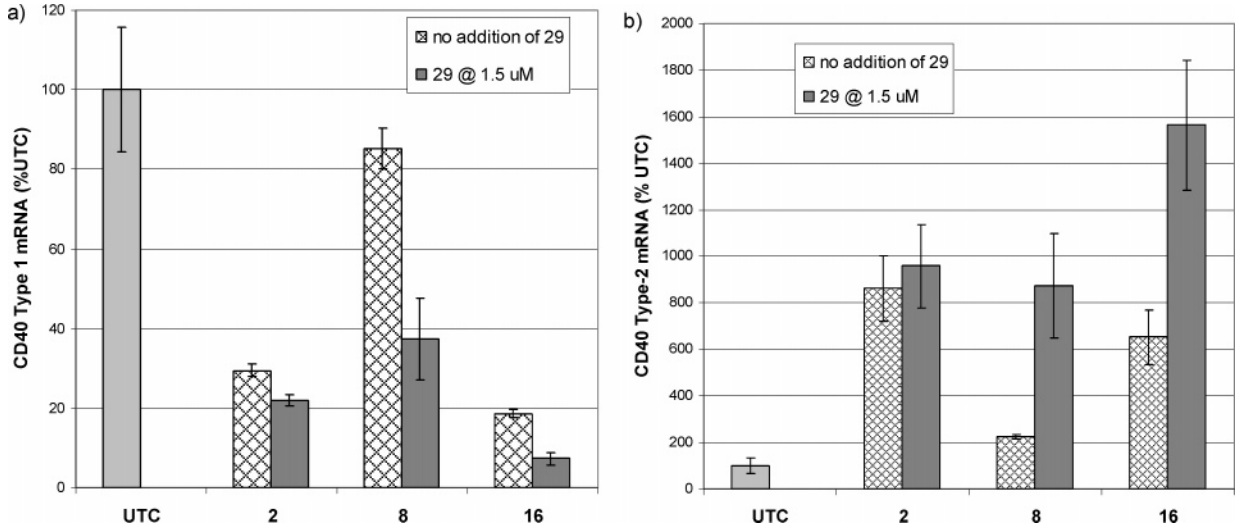

Figure 3. Effect of "off-target" PNA conjugate **29** on (a) reduction of CD40 type 1 mRNA and (b) induction of CD40 type 2 mRNA with antiCD40 PNA conjugates **2** (3.0 μM), **8** (1.0 μM), and **16** (1.0 μM).

same pathway to enter the cells. Cells were briefly preincubated with the "competitor" **29**, followed by the conjugates **2**, **8** or **16** at fixed concentration of 3.0, 1.0, and 1.0 μM, respectively. The antisense activity of the conjugates with and without **29** is depicted in Figure 3. Cytotoxicity became significant at concentrations of **29** of 3 μM and higher, which prevented the evaluation in a broader concentration range.

Interestingly, the presence of the competitor did not reduce but rather enhanced the inhibitory effect of the anti-CD40 conjugates. This is most evident for conjugate **8**, which was essentially inactive at the concentration used (1.0 μM) unless **29** was present. One explanation could be that the cooperative effect of several peptide conjugates and therefore a certain threshold concentration, which depends on the membrane activity of the peptide, is required for efficient cellular uptake and/or endosomal escape. This hypothesis is further strengthened by the steep dose responses observed for most of the conjugates. Alternatively, competition for unspecific binding sites and a concomitant increase in the fraction of "free" inhibitor available for binding to its target could explain the observed increase in activity.

Biodistribution in Mice. The enzymatically stable retro-inverso isomers of the two most promising peptide motifs from opposite ends of the SAR spectrum, **16** bearing the hydrophilic, arginine-rich peptide and **17** containing the more amphipathic, lysine-rich peptide, were evaluated for their PK/tissue distribution in healthy Balb/c male mice. The radiolabeled analogues of **16** and **17** were prepared by introducing ^{3}H-acetyl at the ϵ-amino group of the C-terminal lysine, yielding **30** and **31**, respectively. The stability of this modification has been evaluated previously in mouse plasma and no evidence of deacetylation was found within 24 h.[12]

Table 5 shows the average tissue concentrations after 24 h for iv administration. The distribution of **31**, with the highest concentrations found in liver, kidney, and spleen, appeared very similar to the octa(L-lysine) conjugate **2** reported previously.[12] On the other hand, **30** showed an overall broader distribution with 4-fold higher levels in the liver and even more dramatic increases in lymph nodes, spleen, pancreas, lung, and heart. However, the fraction of total dose recovered was lower for conjugate **31** compared to **30**. Since some tissues, such as fat, brain, and bone marrow as well as the carcass and feces were not included in the analysis, the study did not allow for accurate mass balance, and therefore, the results could not provide a definitive answer regarding the whereabouts of the remaining fraction of **31**. Excretion in urine was found to be below 1% and 2% of the administered dose for **30** and **31**, respectively (Figure 3, Supporting Information).

Table 5. Average Tissue Concentration of PNA−Peptide Conjugates 30 and 31[a]

	concentration (μg·equiv/g)	
tissue	**30**	**31**
liver	43.4 ± 2.3	9.4 ± 1.1
kidney	17.2 ± 2.1	17.4 ± 2.8
spleen	230 ± 56	1.7 ± 0.6
pancreas	6.4 ± 2.2	0.28 ± 0.04
lungs	9.3 ± 1.8	0.11 ± 0.03
MLN[b]	41.3 ± 7.9	2.9 ± 0.3
heart	3.3 ± 2.4	0.12 ± 0.07
skin	0.35 ± 0.07	0.62 ± 0.12
skeletal muscle	0.22 ± 0.05	0.22 ± 0.01
testes	1.5 ± 0.2	0.23 ± 0.02
small intestine	0.80 ± 0.62	0.46 ± 0.07
large intestine	2.7 ± 1.0	0.55 ± 0.03
plasma	0.15 ± 0.03	0.43 ± 0.08

[a] The values shown represent averages ± SD (n = 3) measured 24 h after iv dosing (3 mg/kg). [b] Mesentery lymph nodes.

The results demonstrate that short basic peptides covalently attached to peptide nucleic acids can improve upon their intrinsically poor uptake and PK properties and moderate structural changes in the peptide carrier can evoke significant variations in the tissue distribution of the corresponding conjugates. Whether or not these PK improvements will translate into peptide nucleic acids that are capable of eliciting potent antisense effects in the tissues to which they are delivered remains to be evaluated. While CD40 represents a therapeutically interesting target, its expression is limited to B-lymphocyte, dentritic cell, and macrophage subpopulations of a few tissues such as spleen and lymph nodes. The results from the biodistribution studies indicated that a more broadly expressed target protein would be advantageous to evaluate the in vivo pharmacology of antisense PNA−peptide conjugates and to determine whether such constructs could offer any advantage over existing antisense chemistries. Thus, we developed an antisense PNA against murine PTEN, which is expressed in a wide variety of tissues. Comprehensive PK/PD studies with a selection of promising peptide vectors are currently in progress and will be reported shortly.

Conclusion

A series of cationic amphipathic peptides was designed to investigate the structural features required to promote efficient cellular uptake and elicit antisense activity with a PNA pentadecamer that redirects splicing of murine CD40 transcript. On the basis of an idealized α-helix, the amino acid sequence was altered to cover a range of the helix parameters hydrophobicity and amphipathicity. Two promising motifs emerged from the first tier SAR, one with an extended basic face composed of either lysine or arginine and one with an extended hydrophobic face composed of alanine and leucine. The results emphasized the importance of positive charge as well as amphipathicity. To investigate further the interplay between the two parameters, a second SAR series was designed. The results indicate that the optimal range of amphipathicity between inactivity and cytotoxicity is narrow. The discrepancy between cellular uptake and activity observed for some of the conjugates suggests that intracellular trafficking and specifically nuclear localization are influenced by the nature of the peptide carrier. In primary murine macrophages, the D-isomers of the parent conjugate showed significantly increased uptake and activity, demonstrating the importance of stability against enzymatic attack. The stabilized isomers of the two most promising conjugates were administered to healthy mice. They rapidly distributed to a variety of tissues and showed only modest elimination via excretion within the time frame of the experiment. Substantially higher levels of the arginine-rich conjugate were found in a variety of tissues, demonstrating the influence of the peptide carrier on biodistribution. Our results suggest that conjugation to simple basic peptides not only provides a viable strategy to improve cellular uptake but also serves as a versatile tool for modulating the in vivo biodistribution of antisense PNA.

Experimental Section

Reagents and Solvents. The solvents used were purchased from Aldrich, Burdick & Jackson, or EMD in the highest grade available. Amino acids, the resins used for solid-phase synthesis, HBTU, and HOBt were purchased from Novabiochem. PNA monomers (Boc-protected), HATU, and *N*-Boc-8-amino-3,6-dioxaoctanoic acid were obtained from Applied Biosystems. The fluorescent dye Oregon-Green488 was purchased from Molecular Probes, Invitrogen Corp. Soluene-350 was purchased from Beckman, and Econo-safe was obtained from RPI. Cell culture reagents were obtained from Invitrogen. All other reagents were purchased from Sigma-Aldrich Corp.

Synthesis, Purification, and Characterization of PNA−Peptide Conjugates. For the N-terminal peptide conjugates, the PNA part of the conjugates with the sequence CACAGATGA-CATTAG-Lys (**1**) was assembled on MBHA polystyrene resin, preloaded with Boc-Lys(2-Cl-Z) (loading 175 μmol/g), using a 433 A peptide synthesizer (Applied Biosystems) according to previously published procedures for PNA synthesis.[27,28] The synthesis of the peptide part of the conjugate was carried out manually and in parallel either with Fmoc- or Boc-chemistry using custom-fabricated glass columns equipped with a glass frit, a stopcocked outlet, and an argon inlet. C-terminal peptide conjugates were assembled manually and in parallel using Boc-chemistry throughout the synthesis. Deprotection and cleavage were generally carried out using a low/high TFMSA treatment, and the duration of the treatment was determined by the side chain protecting groups present.

The conjugates were purified by RP-HPLC using a Gilson HPLC system including a 306 piston pump system, a 811C dynamic mixer, a 155 UV/vis detector, and a 215 liquid handler together with Unipoint software on Zorbax SB300 C_3 column (Agilent). Heptafluorobutyric acid (0.1%) in H_2O (A) and CH_3CN (B) were used as the solvent system. The applied gradient was dependent on the length and sequence of the conjugate. Dual wavelength detection was carried out at 220 and 260 nm and the column temperature was kept at 60 °C.

The purified conjugates were analyzed by analytical HPLC (generally the purity was greater 90%) and mass spectrometry (ESI-MS) and stored at −20 °C until prior to use (analytical data for all compounds are listed in the Supporting Information).

Calculation of Helix Parameters. The helical parameters of the peptides were calculated according to Eisenberg et al.[29] on the basis of the hydrophobic parameters obtained from Fauchère and Pliška.[30]

Circular Dichroism Spectroscopy. Circular dichroism (CD) measurements were carried out on a Cary 61 spectopolarimeter that was modified by replacing the original Pockel cell with a 50 kHz photoelastic modulator (Hinds International FS-5/PEM-80). The original Cary linear polarizer was replaced with a MgF_2 linear polarizer supplied by AVIV, Inc. An EGG Princeton Applied Research model 128A lock-in amplifier was used to integrate the phase-detected output of the original end-on PMT and preamp. System automation, multiple scan signal averaging, and baseline subtraction were accomplished with an AT286 PC interfaced directly to both the Cary 61 and the 128A amplifier. The system software and custom hardware interfaces were designed by Allen MicroComputer Services Inc. and the UC San Diego Department of Chemistry & Biochemistry Computer Facility. The CD spectra were obtained using a 0.05−0.5 cm path length cell by signal averaging 10 scans from 185 to 300 nm at a scan speed of 0.8 nm/s. The concentration of PNA conjugates in the samples was between 10 and 20 μM. The solvent buffers used for analysis were 10 mM phosphate (pH 7), 15 mM SDS in 10 mM phosphate (pH 7), 10 mM phosphate (pH 5), or 15 mM SDS in 10 mM phosphate (pH 5).

Preparation of ^{3}H-Acetyl-Labeled PNA−Peptide Conjugates 30 and 31. The PNA−peptide conjugates **16** and **17** were synthesized with a C-terminal Lys(Fmoc) residue. After completion of solid-phase synthesis, the Fmoc-group was removed with 20% piperidine in DMF, and the resin was washed with DMF and DCM and dried in vacuo. Labeling, cleavage, and purification of the compounds was carried out at Moravek Biochemicals (Brea, CA) according to a previously published protocol.[12]

Enzymatic Stability of PNA−Peptide Conjugates. Solutions (10 μM) of the PNA−peptide conjugates in either 10% FBS-containing cell culture medium (RPMI 1640, Gibco, Invitrogen Inc.) or mouse serum stabilized with 10 mM Hepes and diluted to 25% with PBS (pH 7.1−7.4) were prepared and incubated at 37 °C. Analysis of the samples and determination of half-lives were carried out as described previously.[12]

Cells. BCL_1 cells were obtained from the American Type Culture Collection and grown in normal growth medium (Dulbecco's modified Eagle medium, supplemented with 10% fetal bovine serum and antibiotics). Cells were incubated in a humidified chamber at 37 °C, containing 5% CO_2. PNA conjugates were added to cells at the indicated final concentrations. Cells were exposed to compound for 3 days. All experiments were done in triplicate.

Primary thioglycollate-elicited macrophages were isolated by peritoneal lavage from 6−8-week-old female C57Bl/6 mice that had been injected with 1 mL of 3% thioglycollate broth 4 days previously. After overnight incubation with PNA conjugates, primary macrophages were activated by treatment with 100 ng/mL rIFN-γ (R&D Systems) for 4 h and then lysed for total RNA isolation.

Cell Viability. BCL_1 cells were seeded at 2000 cells per well into 96-well plates. Following 3 days of compound exposure, wells were analyzed for relative number of viable cells using the WST-1 assay (Roche) according to manufacturer's protocol. Compound-related effects on cell proliferation and viability were considered to be significant if the average absorbance of WST-1 at a wavelength of 450 nm dropped below 50% of untreated control.

Flow Cytometry Analysis. Cells were detached from culture plates with 0.25% trypsin. Trypsin was neutralized with an equal volume of normal growth medium, and cells were pelleted. Cell pellets were resuspended in 200 μL of staining buffer (phosphate-buffered saline containing 2% bovine serum albumin and 0.2% NaN_3) containing 1 μg of either FITC-labeled isotype control antibody or FITC-labeled anti-CD40 antibody (clone HM40-3, BD Biosciences). Cells were stained for 1 h, washed once with staining buffer, and resuspended in PBS. CD40 surface expression level was determined using a FACScan flow cytometer (Becton Dickinson). Untreated control cells (UTC) lacking PNA treatment were handled identically and also analyzed for CD40 surface expression by flow cytometry.

RT-PCR. Total RNA was isolated using an RNeasy Mini Kit (Qiagen). Real-time quantitative RT-PCR was performed on total RNA from primary macrophages using an ABI Prism 7700. Primer and dual-labeled probe sequences were as follows. Mouse CD40, type 1: forward, 5′-CACTGATACCGTCTGTCATCCCT-3′; reverse, 5′-AGTTCTTATCCTCACAGCTTGTCCA-3′; probe, 5′-FAM-AGTCGGCTTCTTCTCCAATCAGTCATCACTT-TAMRA-3′. Mouse CD40, type 2: forward, 5′-CACTGATACCGTCTGTCAT-CCCT-3′; reverse, 5′-CCACATCCGGGACTTTAAACCTTGT-3′; probe, 5′-FAM-CCAGTCGGCTTCTTCTCCAATCAGTCA-TAM-RA-3′. Mouse CD40: forward, 5′-TGTGTTACGTGCAGTGA-CAAACAG-3′; reverse, 5′-GCTTCCTGGCTGGCACAA-3′; probe, 5′-FAM-CCTCCACGATCGCCAGTGCTGTG-TAMRA-3′. Mouse cyclophilin: forward, 5′-TCGCCGCTTGCTGCA-3′; reverse, 5′-ATCGGCCGTGATGTCGA-3′; probe, 5′-FAM-CCATGGTCAAC-CCCACCGTGTTC-TAMRA-3′. For each sample, mRNA levels were normalized to total RNA, as measured by Ribogreen (Invitrogen).

PK/Tissue Distribution. Radiolabeled conjugates **30** and **31** were administered iv into male Balb/c mice ($n = 3$) at a dose of 3 mg/kg (0.5 mg/mL in PBS with 6% EtOH, pH 7.1). Mice were sacrificed after 24 h, and samples from blood, urine, heart, lung, liver, kidney, spleen, mesentery lymph nodes, pancreas, small/large intestine, testes, skeletal muscle, and furless skin were collected and dissolved in tissue solubilizer (Soluene-350). The samples were then added to liquid scintillation buffer (Econo-safe), and radioactivity was measured in a liquid scintillation counter (Beckman, LS6000IC).

Acknowledgment. The authors thank Donna Witchell, John Matson, Jinsoo Kim, Gina Riley, and An Hong for their help with the biodistribution study in mice.

Supporting Information Available: Tabular analytical data (HPLC and ESI-MS) for PNA−peptide conjugates, representative example of HPLC and ESI-MS analysis data for compound **8**, microscopic images of primary murine macrophages treated with fluorescently labeled PNA−peptide conjugates, CD spectroscopy of compound **27**, and urinary excretion of conjugates **30** and **31**. This material is available free of charge via the Internet at http://pubs.acs.org.

References

(1) Nielsen, P. E.; Egholm, M.; Berg, R. H.; Buchardt, O. Sequence-selective recognition of DNA by strand displacement with a thymine-substituted polyamide. *Science* **1991**, *254*, 1497−1500.
(2) Egholm, M.; Buchardt, O.; Christensen, L.; Behrens, C.; Freier, S. M.; Driver, D. A.; Berg, R. H.; Kim, S. K.; Norden, B.; Nielsen, P. E. PNA hybridizes to complementary oligonucleotides obeying the Watson−Crick hydrogen-bonding rules. *Nature* **1993**, *365*, 566−568.
(3) Demidov, V. V.; Potaman, V. N.; Frank-Kamenetskii, M. D.; Egholm, M.; Buchardt, O. Sonnichsen, S. H.; Nielsen, P. E. Stability of peptide nucleic acids in human serum and cellular extracts. *Biochem. Pharmacol.* **1994**, *48*, 1310−1313.
(4) Knudsen, H.; Nielsen, P. E. Antisense properties of duplex- and triplex-forming PNAs. *Nucleic Acids Res.* **1996**, *24*, 494−500.
(5) Wu, H.; Lima, W. F.; Zhang, H.; Fan, A.; Sun, H.; Crooke, S. T. Determination of the role of the human RNase H1 in the pharmacology of DNA-like antisense drugs. *J. Biol. Chem.* **2004**, *279*, 17181−17189.
(6) Janowski, B. A.; Kaihatsu, K.; Huffman, K. E.; Schwartz, J. C.; Ram, R.; Hardy, D.; Mendelson, C. R.; Corey, D. R. Inhibiting transcription of chromosomal DNA with antigene peptide nucleic acids. *Nat. Chem. Biol.* **2005**, *1*, 210−215.
(7) Siwkowski, A. M.; Malik, L.; Esau, C. C.; Maier, M. A.; Wancewicz, E. V.; Albertshofer, K.; Monia, B. P.; Bennett, C. F.; Eldrup, A. B. Identification and functional validation of PNAs that inhibit murine CD40 expression by redirection of splicing. *Nucleic Acids Res.* **2004**, *32*, 2695−2706.
(8) Grewal, I. S.; Flavell, R. A. CD40 and CD154 in cell-mediated immunity. *Annu. Rev. Immunol.* **1998**, *16*, 111−135.
(9) Noelle, R. J. CD40 and its ligand in host defense. *Immunity* **1996**, *4*, 415−419.
(10) Sazani, P.; Kang, S.-H.; Maier, M. A.; Wei, C.; Dillman, J.; Summerton, J.; Manoharan, M.; Kole. K. Nuclear antisense effects of neutral, anionic and cationic oligonucleotide analogs. *Nucleic Acids Res.* **2001**, *29*, 3965−3974.
(11) Sazani, P.; Gemignani, F.; Kang, S.-H.; Maier, M. A.; Manoharan, M.; Persmark, M.; Bortner, D.; Kole, R. Systemically delivered antisense oligomers upregulate gene expression in mouse tissues. *Nat. Biotechnol.* **2002**, *20*, 1228−1233.
(12) Albertshofer, K.; Siwkowski, A. M.; Wancewicz, E. V.; Esau, C. C.; Watanabe, T.; Nishihara, K. C.; Kinberger, G. A.; Malik, L.; Eldrup, A. B.; Manoharan, M.; Geary, R. S.; Monia, B. P.; Swayze, E. E.; Griffey, R. H.; Bennett, C. F.; Maier, M. A. Structure−activity relationship study on a simple cationic peptide motif for cellular delivery of antisense peptide nucleic acid. *J. Med. Chem.* **2005**, *48*, 6741−6749.
(13) Fischer, P. M.; Krausz, E.; Lane, D. P. Cellular delivery of impermeable effector molecules in the form of conjugates with peptides capable of mediating membrane translocation. *Bioconjugate Chem.* **2001**, *12*, 825−841.
(14) Plank, C.; Zauner, W.; Wagner, E. Application of membrane-active peptides for drug and gene delivery across cellular membranes. *Adv. Drug Del. Rev.* **1998**, *34*, 21−35.
(15) Langel, U. *Cell-penetrating peptides: Processes and applications*; CRC Press: Boca Raton, FL, 2002.
(16) Brooks, H.; Lebleu, B.; Vives, E. Tat peptide-mediated cellular delivery: Back to basics. *Adv. Drug Del. Rev.* **2005**, *57*, 559−577.
(17) Scheller, A.; Oehlke, J.; Wiesner, B.; Dathe, M.; Krause, E.; Beyermann, M.; Melzig, M.; Bienert, M. Structural requirements for cellular uptake of alpha-helical amphipathic peptides. *J. Pept. Sci.* **1999**, *5*, 185−194.
(18) Scheller, A.; Wiesner, B.; Melzig, M.; Bienert, M.; Oehlke, J. Evidence for an amphipathicity independent cellular uptake of amphipathic cell-penetrating peptides. *Eur. J. Biochem.* **2000**, *267*, 6043−6049.
(19) Oehlke, J.; Wallukat, G.; Wolf, Y.; Ehrlich, A.; Wiesner, B.; Berger, H.; Bienert, M. Enhancement of intracellular concentration and biological activity of PNA after conjugation with a cell-penetrating synthetic model peptide. *Eur. J. Biochem.* **2004**, *271*, 3043−3049.
(20) Turner, J. J.; Ivanova, G. D.; Verbeure, B.; Williams, D.; Arzumanov, A. A.; Abes, S. Lebleu, B.; Gait, M. J. Cell-penetrating peptide conjugates of peptide nucleic acids (PNA) as inhibitors of HIV-1 Tat-dependent trans-activation in cells. *Nucleic Acids Res.* **2005**, *33*, 6837−6849.
(21) Tone, M.; Tone, Y.; Fairchild, P. J.; Wykes, M.; Waldmann, H. Regulation of CD40 function by its isoforms generated through alternative splicing. *Proc. Natl. Acad. Sci. U.S.A.* **2001**, *98*, 1751−1756.
(22) Abibi, A.; Protozanova, E.; Demidov, V. V.; Frank-Kamenetskii, M. D. Specific versus nonspecific binding of cationic PNAs to duplex DNA. *Biophys. J.* **2004**, *86*, 3070−3078.
(23) Sitaram, N.; Nagaraj, R. Interaction of antimicrobial peptides with biological and model membranes: Structural and charge requirements for activity. *Biochim. Biophys. Acta* **1999**, *1462*, 29−54.
(24) Kichler, A.; Leborgne, C.; Marz, J.; Danos, O.; Bechinger, B. Histidine-rich amphipathic peptide antibiotics promote efficient delivery of DNA into mammalian cells. *Proc. Natl. Acad. Sci. U.S.A.* **2003**, *100*, 1564−1568.
(25) Fischer, R.; Koehler, K.; Fotin-Mleczek, M.; Brock, R. A stepwise dissection of the intracellular fate of cationic cell-penetrating peptides. *J. Biol. Chem.* **2004**, *279*, 12625−12635.
(26) Nigg, E. A. Nucleocytoplasmic transport: Signals, mechanisms and regulation. *Nature* **1997**, *386*, 779−787.
(27) Christensen, L.; Fitzpatrick, R.; Gildea, B.; Petersen, K. H.; Hansen, H. F.; Koch, T.; Egholm, M.; Buchardt, O.; Nielsen, P. E.; Coull, J.; Berg, R. H. Solid-phase synthesis of peptide nucleic acids. *J. Pept. Sci.* **1995**, *1*, 185−183.

(28) Koch, T.; Hansen, H. F.; Andersen, P.; Larsen, T.; Batz, H. G.; Otteson, K.; Orum, H. Improvements in automated PNA synthesis using Boc/Z monomers. *J. Pept. Res.* **1997**, *49*, 80−88.
(29) Eisenberg, D.; Weiss, R. M.; Terwilliger, T. C. The hydrophobic moment detects periodicity in protein hydrophobicity. *Proc. Natl. Acad. Sci. U.S.A.* **1984**, *81*, 140−144.
(30) Fauchere, J.-L., Pliska, V. Hydrophobic parameters π of aminoacid side chains from the partitioning of *N*-acetyl-aminoacid amides. *Eur. J. Med. Chem.—Chim. Ther.* **1983**, *18*, 369−375.

JM051275Y